Journal of Alloys and Compounds 293–295 (1999) 472–475

Pd-cluster size effects of the hydrogen sorption properties

A. Züttel[a,*], Ch. Nützenadel[a], G. Schmid[b], D. Chartouni[a], L. Schlapbach[a]

[a]*University of Fribourg, Physics Institute, Pérolles, CH-1700 Fribourg, Switzerland*
[b]*Instit für Anorganische Chemie, Universität-GH Essen, D-45115 Essen, Germany*

Abstract

Clusters are agglomerates of a few to some hundred atoms. A large fraction of the atoms find themselves on a surface site. The geometrical structure of a cluster, in contrast to the structure of crystalline bulk material, can not be described with a repeated, a space filling unit cell. Clusters appear often in regular geometrical polyhedrons e.g. cuboctahedron or icosahedron. The interaction between hydrogen and palladium clusters of different sizes was investigated. The sorption properties of the clusters are compared with the well known properties of Pd bulk material. The Pd clusters reversibly absorb and desorb hydrogen. The density of states (DoS) distribution of hydrogen in the Pd cluster becomes wide with decreasing cluster size. This is an indication for a lowering of the critical temperature for the hydride formation of small Pd clusters.

Keywords: Palladium; Cluster size; Hydrogen sorption

1. Introduction

Clusters are agglomerates of a few hundred to a few thousand particles (atoms) with a radius smaller than 50 nm. Clusters are grown in the gas phase or vacuum (supersonic jets, gas aggregation, and surface erosion), by electrochemical deposition on an electrode surface, by reduction of metal ions in a solution, or by evaporation on a substrate (islands).

Palladium is a noble metal and has a high hydrogen storage capacity (O.6 H/Pd). Pd-Clusters were evaporated in vacuum on a graphite (HOPG) substrate [2]. We observed those clusters in an electrochemical cell (6 mol KOH) in-situ during hydrogen absorption (charging) with a non-contact atomic force microscopy (AFM) [3]. The clusters increased in size after a voltage has been applied in order to charge them with hydrogen. This size increase proves that palladium clusters intercalate hydrogen similar to the Pd bulk material.

Metal clusters evaporated on a substrate usually show a wide size distribution. Properties which are determined from such a cluster sample are always averaged over a large range in cluster size. In order to investigate size-dependent properties of the clusters either single isolated clusters or cluster samples with a very narrow size distribution were examined.

Large clusters samples (≈1 g) of some noble elements, e.g. Pd, with a narrow size distribution were synthesized [5] by the reduction of the metal ions with hydrogen gas in a solution of Pd^{II}-acetate. The metal atoms form a cluster and organic ligands bind to the surface of the cluster. The ligand shell (e.g. phenantroline) stabilizes the clusters and prevents cluster agglomeration. By simple drying in air stable black cluster-powder is achieved.

The ligand-stabilized clusters have several advantages over the electrochemically deposited clusters: (1) the cluster samples have a narrow size distribution, i.e. nearly all the clusters are of the same size; (2) the cluster powder is stable and easy to handle; (3) the ligands can easy be removed (ligands desorb at 50°C), (4) the clusters are separated from each other by the ligands and (5) large samples can be produced.

The structural and hydriding properties of three mono-dispersed cluster samples $P^{7/8}$ (95% of 7 shell clusters and 5% of 8 shell clusters), Pd^5 (5 shell clusters), Pd^2 (2 shell clusters) and Pd bulk powder (particle size≈50 μm) are compared in this work (Table 1).

2. Structure of Pd-clusters

The growth mechanism of clusters of ideal spherical atoms was calculated by Northby [7,8]. Starting with two single atoms a dimer, $N=2$ is formed. The trimer, $N=3$, has the geometry of an equilateral triangle; $N=4$ corre-

---

*Corresponding author. Tel.: +41-26-300-9086; fax: +41-26-300-9747.

0925-8388/99/$ – see front matter
PII: S0925-8388(99)00467-3

Table 1
Parameters of the cluster samples: composition, abbreviation, number of shells, calculated diameter, full with at half maximum (FWHM) of the main X-ray diffraction peak

Cluster		n_s	d [nm]	FWHM
$Pd_{55}phen^*_{36}O_{30}$	Pd^2	2	1.0	5.70
$Pd_{561}phen^*_{36}O_{200}$	Pd^5	5	2.6	1.83
$Pd_{1415}phen^*_{60}O_{1100}$, $Pd_{2057}phen^*_{20}O_{1600}$	$Pd^{7/8}$	7/8	3.7..4.2	1.45
Pd powder (≈50 μm)	Pd^{∞}	fcc	50 000	0.40

sponds to a tetrahedron, $N=5$ to a triangular bipyramide. For $N=7$ the cluster appears as a pentagonal bipyramide, i.e. a ring of five atoms, with one atom above and one below it. The smallest member of the clusters with icosahedral geometry is observed for $N=13$, one interior atom with two pentagonal caps, i.e. an icosahedron (Fig. 1). Pentagonal (five-fold) symmetry is not space-filling and therefore does not occur in infinite lattices. The number of nearest neighbors in an icosahedron is larger than in a fcc lattice and the surface energy is smaller (smaller surface-to-volume-atom ratio) compared to the fcc lattice, that is the reason for the stability of the icosahedral shaped clusters. The icosahedron can be constructed from 20 slightly distorted fcc unit cells, whose faces are (111) planes and which share common vertex. The interatomic spacing is not uniform in an icosahedron. This leads to a built-up of mechanical stresses, so that for large N ($N \geq 1500$) the fcc lattice becomes favored.

The growth of larger clusters ($N \geq 13$) can be interpreted in terms of shell models. This model is based on the assumption that clusters of particular sizes have structures that correspond to closed shells of component particles. Clusters are relatively more stable if the number of atoms in clusters with an icosahedral geometry is a magic number (13, 55, 147, 309, 561 . . .) [6]. The smallest possible icosahedral cluster consists of 13 atoms, one in the center and 12 others on each of the 12 equivalent corners of the icosahedron. An icosahedron consists of 20 faces, 30 edges and 12 corners. The number of atoms in a cluster (N_V) with an icosahedron geometry is calculated according to

$$N_V = 1 + 2 \cdot n + \frac{5}{3} \cdot \{n \cdot (n+1) \cdot (2n+1)\}$$

$$\text{for } n \geq 1 \quad \text{Magic numbers}$$

where (n) is the number of shells of the cluster. The number of atoms at the surface of the cluster (N_S) is equal to the number of atoms in the latest shell

$$N_S = 12 + 10 \cdot (n-1) \cdot (n+1) \quad \text{for } n \geq 1 \quad \text{Surface atoms}$$

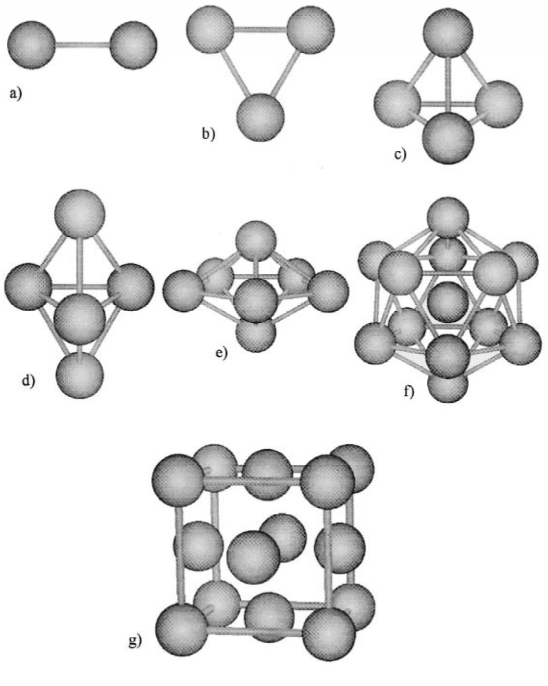

Fig. 1. Growth sequence to form icosahedral clusters: (a) dimer, (b) trimer, (c) tetrahedron, (d) triangular bipyramide, (e) pentagonal bipyramide, (f) icosahedron, (g) face centered cubic (fcc) structure (s.g. Fm-3m, #225).

The X-ray diffraction patterns (Cu K_α, $\lambda_1 = 1.540562$ Å, $\lambda_2 = 1.544390$ Å, $I_2/I_1 = 0.5$) of bulk Pd and the three cluster samples $Pd^{7/8}$, Pd^5 and Pd^2 are shown in Fig. 2. Bulk Pd crystallizes in a face centered cubic (fcc) structure (s.g. Fm-3m, #225) with the lattice parameter $a = 3.889(2)$ Å ($T = 298$ K).

The three cluster samples $Pd^{7/8}$, Pd^5 and Pd^2 exhibit diffraction peaks at the same position as bulk Pd and therefore the lattice parameters calculated from the refinement [7,8] of the diffraction pattern are the same for the cluster samples and bulk Pd within the accuracy of the calculation. However, the full width at half maximum (FWHM) of the main diffraction peaks is inversely proportional to the size of the cluster (Table 1).

$$\text{FWHM} = 5° \text{ nm d}^{-1} \quad \text{Peak width}$$

The small size [9] as well as the mechanical stress in the cluster leads to peak broadening. There are indications that the outer most shell of an icosahedral cluster is closer to the second most outer shell than all the other inter-shell distances [10,11].

3. Pd-cluster–hydrogen interaction

Small samples (≈0.2 g) of the Pd-clusters were hydrided and dehydrided with hydrogen gas. The X-ray diffraction pattern of the clusters was checked before and after the hydrogenation. No changes in the diffraction pattern were observed between the samples before and after the hydrogen absorption/desorption cycle. This is a proof for the stability of the Pd-clusters upon hydrogenation.

Small Pd-cluster samples (20 mg) were mixed with copper powder (80 mg) and pressed (500 MPa) to a pellet (7 mm in diameter). The pellets were used as electrodes in

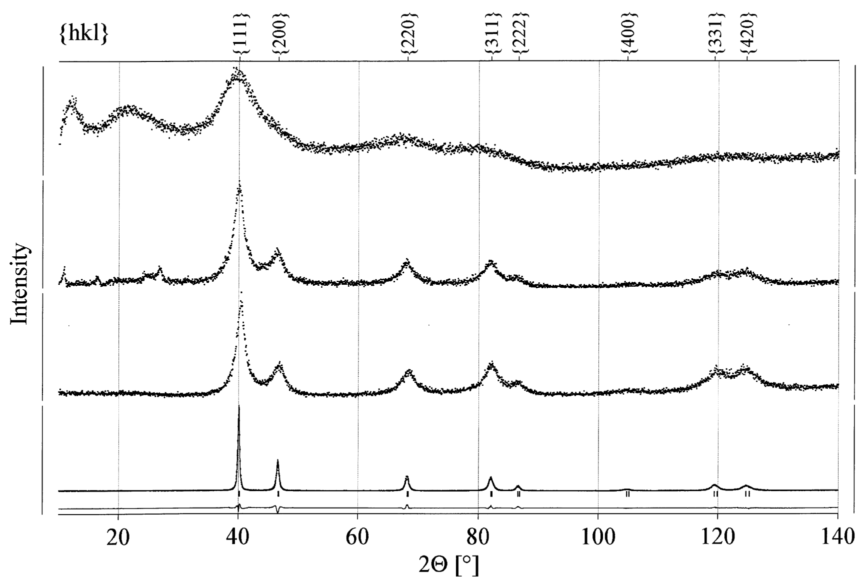

Fig. 2. X-ray diffraction patterns (from top to bottom): Pd^2 (2 shells), Pd^5 (5 shells), $Pd^{7/8}$ (7/8 shells), Pd powder (particle size = 50 μm), position of the diffraction lines in fcc Pd and difference between the measured intensities and the fit for bulk Pd.

an alkaline electrochemical half-cell. The electrodes were charged and discharged with constant current pulses and the equilibrium potential was measured versus a Hg/HgO reference electrode in the pauses between the pulses. The electrochemical equilibrium potential ($AB^0 = \Delta E^0 = \Delta E_{eq} - \Delta E_{Hg/HgO}$) [12] is directly related to the equilibrium gas phase pressure (p_{eq}) and to the Gibb's free energy (ΔG)

$$\Delta G = -\Delta E^0 \cdot n \cdot F = R \cdot T \cdot \ln\left(\frac{p_{eq}}{p_0}\right)$$
$$= \Delta H(T) - T \cdot \Delta S \quad \text{Gibb's free energy}$$

where n stands for the number of transferred electrons $n = 2$, F for the Faraday constant $F = 96494$ As mol^{-1}, R for the gas constant $R = 8.3\ 14$ J mol^{-1} K^{-1}, T for the temperature in Kelvin, ΔS for the enthalpy of the reaction and ΔS for the entropy of the reaction ($\Delta S \approx 120$ J mol^{-1} K^{-1}). Therefore, the electrochemical potential is a direct measure of the chemical potential of the hydrogen in the sample. Fig. 3 shows the density of states for hydrogen (DoS) as a function of the equilibrium potential (ΔE^0), i.e. the first derivative of the hydrogen concentration over the equilibrium potential. Bulk Pd exhibits a narrow DoS distribution. With decreasing size of the clusters the width of the DoS distribution increases. Furthermore, the distance between the maximum in the DoS distribution for absorption and desorption increases with decreasing cluster size. In the size range from 7/8 shells to 2 shells the hydrogen sorption properties are strongly size dependent. The pronounced phase transition from Pd to $PdH_{0.6}$ which is found for bulk Pd is still observed in the cluster samples, however in a less clear form. The increasing width of the DoS distribution is also observed for bulk Pd at elevated temperatures, i.e. close to the critical temperature (T_c (bulk Pd) = 571 K [13]). The critical temperature for the hydride formation of the clusters is probably size dependent and decreases with decreasing cluster size.

The capacity decreases with decreasing cluster size. Hydrogen usually occupies tetrahedral or octahedral inter-

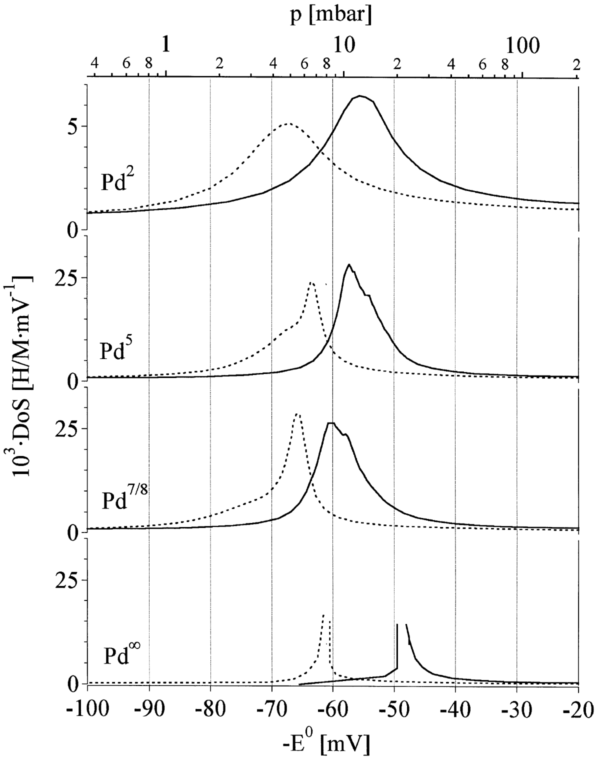

Fig. 3. DoS (density of states) for hydrogen calculated from the concentration vs. the equilibrium potential curve for bulk Pd, $Pd^{7/8}$ cluster, Pd^5 cluster, and Pd^2 (from bottom to top). Solid lines represent the absorption and broken lines the desorption.

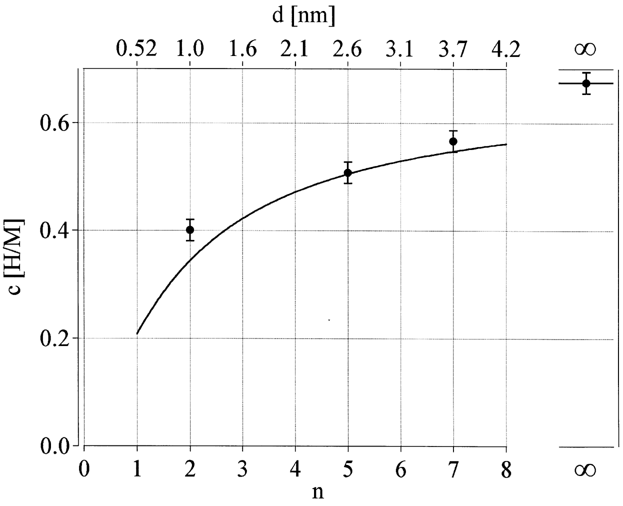

Fig. 4. Hydrogen capacity as a function of the number of shells in the Pd clusters. The line represents the calculated capacity and the markers stand for the measured capacities. Bulk Pd is placed at an infinite number of shells. 100% of capacity corresponds to $PdH_{0.67}$ (H/M = 0.67, 170 mAh/g).

stitial sites in the host metal. A fcc structure offers 1 octahedral and 2 tetrahedral interstitial sites per metal atom for hydrogen. By the simple assumption that surface atoms provide less interstitial sites for hydrogen, the capacities for different cluster sizes were calculated: at corners 0.25 H/M (H atoms per metal atom), at edges 0.4 H/M and at faces 0.5 H/M.

$$C[\mathrm{H}] = 0.6 \cdot \left\{ 4 + (n-1) \cdot \left(4 + \frac{10}{3} \cdot n \cdot (n+1) \right) \right\}$$

Hydrogen capacity of Pd-clusters

where n is the number of shells in the Pd-cluster and $C[\mathrm{H}]$ the capacity in hydrogen-atoms for the hole cluster with n shells.

Fig. 4 shows the calculated capacities according to the model as well as the four measured capacities for Pd bulk powder (particle size = 50 μm), $\mathrm{Pd}^{7/8}$ clusters, Pd^{5} cluster and Pd^{2} clusters. The measured and the calculated capacities are in good agreement.

4. Conclusion

Palladium clusters in the size range of 55 atoms (1 nm) up to bulk Pd (50 μm) were investigated. A closed shell model (cuboctahedra, icosahedra) describes the structure and the size of the clusters, however, the broad diffraction peaks in the X-ray pattern occur at the same position as for fcc Pd. The Pd clusters reversibly absorb and desorb hydrogen. The DoS distribution of hydrogen in the Pd clusters becomes wide with decreasing cluster size. This is an indication of a lowering of the critical temperature for the hydride formation of Pd clusters.

5. Uncited References

[1,4].

Acknowledgements

Financial support by the Swiss priority program (SPP: MINAST) and the great technical support from Elmar Mooser and Francis Bourqui are acknowledged.

References

[1] E. Boschung, C. Nutzenadel, G. Dietler, L. Schlapbach, Hydrogenation of palladium clusters; poster presentation at the workshop of nanoscience, Hasliberg, August 1996.

[2] C. Nützenadel, A. Züttel, D. Chartouni, L. Schlapbach, Nanosized Batteries; poster presentation at the workshop of nano science, Hasliberg, August 1996.

[3] G. Schmid, J. Am. Chem. Soc. 115 (1993) 2046.

[4] G. Schmid, J. Mol. Cat. A: Chem. 107 (1996) 95.

[5] J.A. Northby, J. Chem. (1987), p. 6166.

[6] A.L. Mackay, Acta Cryst. 15 (1962) 916.

[7] F. Izumi, in: R.A. Young (Ed.), The Rietveld Method, Oxford University Press, Oxford, 1993, Chap. 13.

[8] Y.-I. Kim, F. Izumi, J. Ceram. Soc. Jpn. 102 (1994) 401.

[9] Geometrically the diameter of the icosahedron surrounding sphere, i.e. the Pd cluster diameter is calculated according to the equation $d = n \cdot a_{\mathrm{fcc}} \cdot 0.5 \cdot \mathrm{sqrt}(5 + \mathrm{sqrt}(5))$ where a_{fcc} stands for the lattice parameter of fcc palladium and n for the number of shells.

[10] J. Farges, M.F. de Feraudy, B. Raoult, G. Torchet, J. Chem. Phys. 78 (1983) 5067.

[11] J.W. Lee, G.D. Stein, J. Chem. Phys. 91 (1987) 2450.

[12] N.V. Smith, Phys. Rev. B 10 (8) (1974) 3197.

[13] E. Wicke, H. Brodowsky, in: G. Alefeld, J. Völkl, (Eds.), Hydrogen in Metals, vol. 2, Chap. 3, Springer-Verlag, 1978, p. 81.